A&A 488, 619–622 (2008)
DOI: 10.1051/0004-6361:200810205


Astronomy & Astrophysics

# The magnetic field of the proto-planetary nebula candidate IRAS 19296+2227

W. H. T. Vlemmings[1] and H. J. van Langevelde[2,3]

[1] Argelander Institute for Astronomy, University of Bonn, Auf dem Hügel 71, 53121 Bonn, Germany
e-mail: wouter@astro.uni-bonn.de
[2] Joint Institute for VLBI in Europe, Postbus 2, 7990 AA Dwingeloo, The Netherlands
[3] Sterrewacht Leiden, Leiden University, Niels Bohrweg 2, 2333 CA Leiden, The Netherlands

Received 16 May 2008 / Accepted 24 June 2008

**ABSTRACT**

*Context.* Magnetic fields are thought to be one of the possible mechanisms responsible for shaping the generally spherical outflow of evolved stars into often aspherical planetary nebulae. However, direct measurements of magnetic fields during the transition to the planetary nebula phase are rare.
*Aims.* The aim of this project is to expand the number of magnetic field measurements of stars in the (proto-)planetary nebula phase and find if the magnetic field strength is sufficient to affect the stellar outflow.
*Methods.* We used Very Long Baseline Array observations to measure the circular polarization due to the Zeeman splitting of 22 GHz $H_2O$ masers in the envelope of the proto-planetary nebula candidate star IRAS 19296+2227 and the planetary nebula K3-35.
*Results.* A strong magnetic field of $B_{\parallel} = -135 \pm 28$ is detected in the $H_2O$ maser region of the proto-planetary nebula candidate IRAS 19296+2227. The $H_2O$ masers of K3-35 are too weak to detect circular polarization although we do present the measurements of weak linear polarization in those masers.
*Conclusions.* The field measured in the masers of IRAS 19296+2227 is dynamically important and, if it is representative of the large scale field, is an important factor in driving the stellar mass loss and shaping the stellar outflow.

**Key words.** masers – stars: magnetic fields – polarization – stars: circumstellar matter – stars: late-type

## 1. Introduction

At the end of their evolution, a majority of stars go through a period of high mass loss that is an important source for replenishing interstellar space with processed materials. During the asymptotic giant branch (AGB) phase, this mass loss produces circumstellar envelopes which are found to undergo a major modification during the rapid transition from AGB star to Planetary Nebula (PN). The standard assumption is that the initial slow AGB mass loss in a short time changes into a fast superwind generating shocks and accelerating the surrounding envelope (Kwok et al. 1978). However, a large fraction of PNe have asymmetric shapes, with the majority of the young PNe being bipolar. Thus, at some point during the evolution to a PNe the AGB stars must undergo a process in which the spherically symmetric outflow is altered to produce a-spherical PNe morphologies. It has been shown that the energy contained in the outflows of young bipolar PNe is often orders of magnitude larger than can be provided by radiation pressure (Bujarrabal et al. 2001). The source of this energy has been argued to be magnetic fields, binary or disk interaction or a combination of these (see e.g. Balick & Frank 2002; Frank et al. 2007, and references therein).

Maser polarization observations are the predominant source of information about the role of magnetic fields during the late stages of stellar evolution. Most observations have focused on the masers in the envelopes of AGB stars, as OH, $H_2O$ and SiO masers are fairly common in these sources, and have revealed strong magnetic fields throughout the entire envelope (e.g. Etoka & Diamond 2004; Vlemmings et al. 2005; Herpin et al. 2006). Because they are a short-lived (≈1000 yr) transition phase between AGB star and PNe, proto-planetary nebulae (PPNe) are fairly rare. However, OH maser observations reveal similar strength magnetic fields as in their progenitor AGB stars (e.g. Bains et al. 2003, 2004). Additionally, a very small fraction of the PPNe maser stars show highly collimated $H_2O$ maser jets. Currently 11 of these so-called "water-fountain" sources have been identified, and they are likely the progenitor of bipolar PNe (Imai 2007, and references therein). Polarization observations of the $H_2O$ masers of W43A have recently revealed that the maser jet is magnetically collimated (Vlemmings et al. 2006b).

Here we present the detection of a strong magnetic field in the $H_2O$ maser region of the circumstellar envelope of the PPNe candidate IRAS 19296+2227, only the second such detection in an object beyond the AGB phase. Additionally, we shortly describe the measurement of linear polarization of the $H_2O$ masers of the PNe K3-35 (Miranda et al. 2001), which was observed together with IRAS 19296+2227. The PNe K3-35 is only one of 4 PNe towards which $H_2O$ masers have been detected (Suárez et al. 2007). IRAS 19296+2227 is a source with both $H_2O$ and OH maser emission and IRAS colors indicative of an AGB star with strong mass loss. Its near kinematic distance is estimated by Engels (1996) to be 3.2 ± 1.3 kpc, which implies an infrared luminosity of 5000 $L_\odot$. Although this luminosity is consistent with that of an AGB star, its maser properties are atypical since both the OH and $H_2O$ spectra are narrow compared with the maser spectra of OH/IR stars. However, its maser properties do resemble those of a number of PPNe candidates. Therefore,

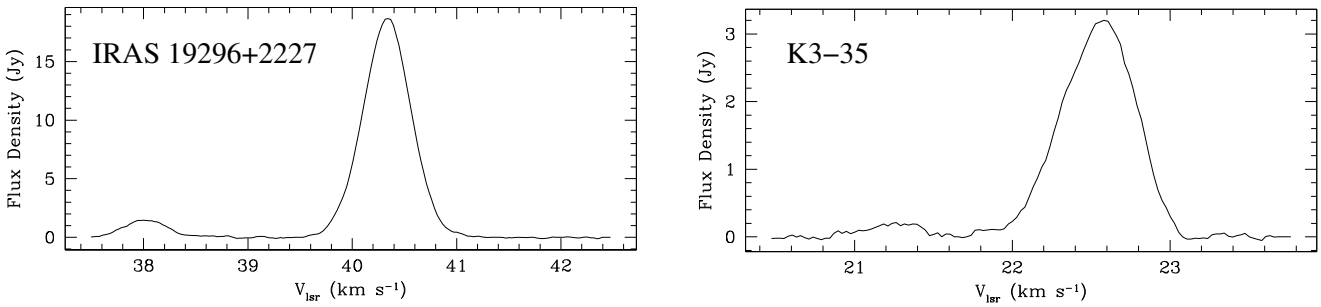


**Fig. 1.** Observed VLBA spectra as measured in the image plane of the $H_2O$ masers of IRAS 19296+2227 (*left*) and K3-35 (*right*).

Engels (1996) concluded that IRAS 19296+2227 should also be considered a PPNe candidate.

## 2. Observations

The NRAO[1] Very Long Baseline Array (VLBA) was used on June 20 2003 to observe the $H_2O$ masers of the PNe K3-35 and PPNe candidate IRAS 19296+2227. The average beam width is $\approx 1.0 \times 0.3$ mas and $1.0 \times 0.7$ mas at the frequency of the $6_{16}-5_{23}$ rotational transition of $H_2O$, 22.235 GHz for IRAS 19296+2227 and K3-35 respectively. We used 4 baseband filters of 1 MHz width, which were overlapped to get a velocity coverage of $\approx 44$ km s$^{-1}$. However, for both sources maser emission was only detected in one of the observing bands. The data were correlated multiple times. The initial correlation was performed with modest (7.8 kHz = 0.1 km s$^{-1}$) spectral resolution, which enabled us to generate all 4 polarization combinations (RR, LL, RL and LR). Two additional correlator runs were performed with high spectral resolution (1.95 kHz = 0.027 km s$^{-1}$) which therefore only contained the two polarization combinations RR and LL. Such high resolution is needed to detect the circular polarization pattern of the $H_2O$ masers at sufficient accuracy. Each source-calibrator pair was observed for 6 h. The calibrator was observed for 1.5 h in a number of scans equally distributed over the 6 h.

### 2.1. Calibration

The data analysis path is described in detail in Vlemmings et al. (2002). It follows the method of Kemball et al. (1995) and was performed in the Astronomical Image Processing Software package (AIPS). The calibration steps were performed on the data-set with modest spectral resolution. Delay and bandpass calibration were done using the calibrator sources J1850 + 2825 and 3C 84, while fringe fitting and self-calibration were performed on a strong maser feature. The calibration solutions were then copied and applied to the high spectral resolution data-set. Finally, corrections were made for instrumental feed polarization using the unpolarized calibrator 3C 84. Unfortunately, no good calibrator data was available for the polarization angle calibration, making it impossible to properly determine the direction of the linear polarization vectors.

The resulting noise in emission free channels of the modest spectral resolution $I$, $Q$, and $U$ data cubes was ~4.0 mJy Beam$^{-1}$ while that in the high spectral resolution $I$ and $V$ cubes was ~8.2 mJy Beam$^{-1}$. In the channels with strong maser emission, the noise increased by ~10%.

[1] The National Radio Astronomy Observatory (NRAO) is a facility of the National Science Foundation operated under cooperative agreement by Associated Universities, Inc.

Figure 1 shows the $H_2O$ maser spectra for IRAS 19296+2227 and K3-35 as measured in the image plane. The high-spectral resolution stokes I image cubes were analyzed using the *AIPS* task SAD, which was used to fit all maser features with peak flux densities higher than 8 times the rms in the channel map with two-dimensional Gaussian components. Subsequently, we only retained components that were detected in at least 10 consecutive channels, corresponding in total to ~0.27 km s$^{-1}$, as narrower features are unlikely to be real. To enable the most accurate positional comparison with the observations in Marvel & Boboltz (1999) we then also determined the mean right ascension and declination off-sets with respect to the reference feature using a flux density-squared weighting scheme. The peak flux, full-width half-maximum ($\Delta v_L$) and velocity ($V_{LSR}$) were determined by fitting a Gaussian to the feature spectra.

## 3. Results

The result of our analysis of the $H_2O$ masers features around IRAS 19296+2227 and K3-35 is presented in Table 1. Here we list the feature LSR velocity, full-width half-maximum ($\Delta v_L$) and the right ascension and declination positional offsets from the maser reference features ($\Delta\alpha$ and $\Delta\delta$). A map of the maser distribution of IRAS 19296+2227 is shown in Fig. 3. Circular polarization of $1.1 \pm 0.2\%$ was detected for the strongest maser ($f$) of IRAS 19296+2227 and its spectrum is shown in Fig. 2. No circular polarization was detected for the weaker features of K3-35. On the other hand, linear polarization at a level of $1.6 \pm 0.2\%$ was only detected on feature $b$ of K3-35 while no significant linear polarization was detected for IRAS 19296+2227.

The relation between circular polarization fraction $P_V$, magnetic field strength along the line of sight $B_\parallel$ and maser line width $\Delta v_L$ is given by $P_V = 2A_{FF'}B_\parallel/\Delta v_L$. However, the coefficient $A_{FF'}$ is a function of maser saturation level and for our analysis of the circular polarization of IRAS 19296+2227 $f$ we used the full radiative transfer non-LTE interpretation described in Vlemmings et al. (2002) to take this into account. In this interpretation, the coupled equations of state of the three dominant hyperfine components of the 22 GHz $H_2O$ maser transition was solved, following Nedoluha & Watson (1992), for a linear maser in the presence of a magnetic field. It is then possible to fit the total intensity and circular polarization spectra directly to model spectra for different intrinsic maser thermal line widths ($\Delta v_{th}$). The emerging maser flux densities of the model spectra are expressed in $T_b\Delta\Omega$, where $T_b$ is the brightness temperature (in K) and $\Delta\Omega$ the beaming solid angle (in sr). The uncertainties in these fits are further discussed in Vlemmings et al. (2006a). The best fit model to the IRAS 19296+2227 spectrum gives $B_\parallel = -135 \pm 28$ mG, $\Delta v_{th} = 1.0 \pm 0.3$ km s$^{-1}$ and $\log(T_b\Delta\Omega) = 9.4 \pm 0.4$.

**Table 1.** Results.

| Name | Feature | Flux ($I$) (Jy beam$^{-1}$) | $V_{\rm rad}$ (km s$^{-1}$) | $\Delta v_{\rm L}$ (km s$^{-1}$) | $\Delta\alpha^a$ (mas) | $\Delta\delta^a$ (mas) | $B_{\parallel}$ (mG) | $m_l$ (%) |
|---|---|---|---|---|---|---|---|---|
| IRAS 19296+2227 | a | 0.54 | 38.04 | 0.41 | 6.18 | –11.07 | | |
| | b | 0.11 | 38.64 | 0.38 | 3.49 | –6.37 | | |
| | c | 0.08 | 40.07 | 0.51 | –16.73 | 3.86 | | |
| | d | 1.70 | 40.28 | 0.59 | 0.88 | –0.30 | | |
| | e | 0.24 | 40.30 | 0.46 | 0.46 | –1.12 | | |
| | f | 8.13 | 40.33 | 0.48 | 0.00 | 0.00 | –135 ± 28 | |
| | g | 0.07 | 40.34 | 0.33 | –1.55 | –2.23 | | |
| | h | 0.18 | 40.75 | 0.64 | –16.04 | 4.99 | | |
| K3-35 | a | 0.22 | 21.26 | 0.40 | 14.00 | 8.70 | | |
| | b | 0.23 | 22.16 | 0.33 | 5.54 | 3.55 | | 1.6 ± 0.2 |
| | c | 3.47 | 22.58 | 0.50 | 0.00 | 0.00 | | |

[a] Positional offsets measured from the maser reference features IRAS 19296+2227$f$ and K3-35$c$.

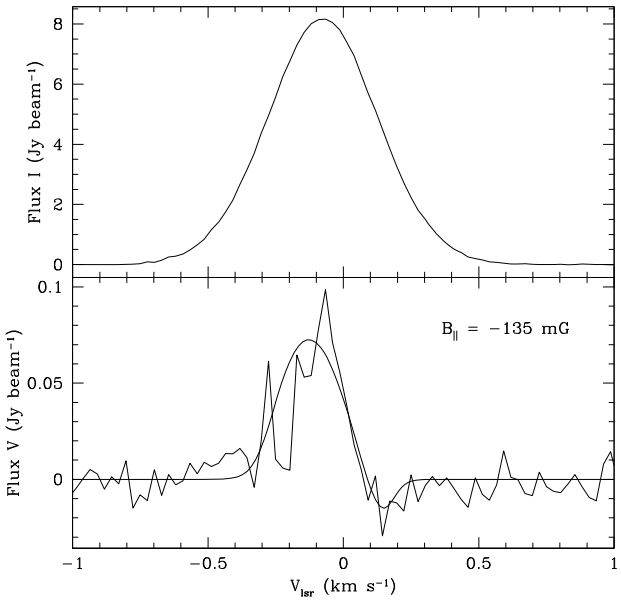


**Fig. 2.** Total power ($I$) and circular polarization ($V$)-spectrum for the strongest maser feature ($f$) of IRAS 19296+2227. The thick solid line in *the bottom panel* shows the best model fit to $V$. This fit corresponds to a magnetic field strength of −135 mG along the maser line-of-sight.

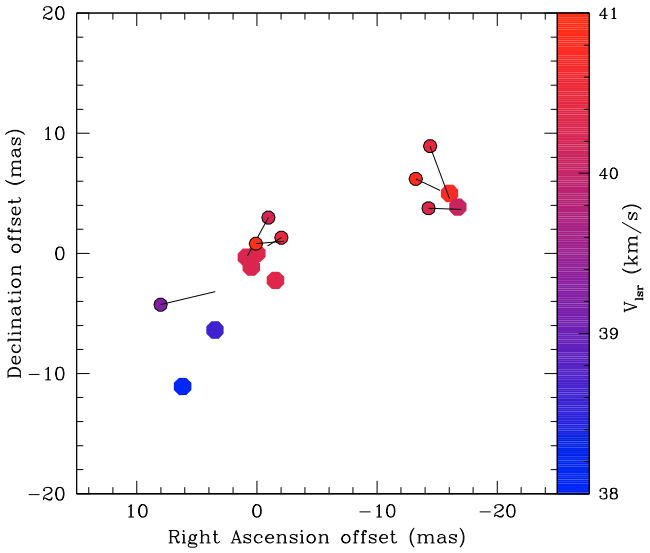


**Fig. 3.** The $H_2O$ maser region of IRAS 19296+2227. The large filled octagons are the maser features detected in our observations and are color-coded according to LSR velocity. The smaller circles with black edges and vectors denote the predicted positions when transposing the maser features with proper motion determinations from Marvel & Boboltz (1999) between May 31, 1997 and June 20, 2003. The vectors indicate the maser feature trajectory, ending at the 1997 positions. This illustrates that the large scale maser proper motions are significantly less than determined in Marvel & Boboltz (1999).

## 4. Discussion

### 4.1. The $H_2O$ maser shell of IRAS 19296+2227

The distribution of the $H_2O$ maser features around IRAS 19296+2227 is shown in Fig. 3. The masers lie in an elongated structure with a length of ∼40 mas. At a distance of 3.2 kpc, this corresponds to a linear size of ∼130 AU. As no larger structure was found in VLA observations (Marvel & Boboltz 1999), this is likely the full extent of the $H_2O$ maser shell.

Marvel & Boboltz (1999) published the first VLBA images made at 3 epochs of observations in 1997 (May 31, June 17 and July 10). Comparing our data with the earlier observations, we find that, while the flux has decreased by more than a factor of two, the maser distribution is extremely similar. Our observations fail to detect several of the weak features at $V_{\rm LSR} > 41$ km s$^{-1}$ but the two most prominent maser groups identified in Marvel & Boboltz (1999) have persisted for over 6 years. Still, the center velocity of some of the maser features, such as the strongest reference feature, has drifted by ≈0.2 km s$^{-1}$, making it impossible to match up individual maser features. As a result, direct proper motion measurements cannot be made. If the maser motions detected by Marvel & Boboltz (1999) are the genuine large scale motions, one expects, after 6 years of motion, a significantly different maser distribution. Figure 3 indicates the positions of the maser features for which proper motions were determined in Marvel & Boboltz (1999), transposed over 6 years. Assuming the maser reference feature was the same in all observational epochs, the predicted maser distribution fails to match our observed distribution, implying that the proper motions determined in Marvel & Boboltz (1999) are likely dominated by random motions of the maser features. Assuming the maser features $c$ and $h$ in our observations originate from the maser clump located at −16.1 and 4.5 mas Right Ascension and Declination off-set respectively in epoch 1 of

Marvel & Boboltz (1999), the maximum proper motion of these features is ∼0.15 mas yr$^{-1}$ which corresponds to ∼2.3 km s$^{-1}$.

As described above, the combined analysis of the total intensity and circular polarization spectra provides additional information on the intrinsic conditions in the maser region. The best fit intrinsic thermal line width of the material that gives rise to the IRAS 19296+2227 $H_2O$ masers was found to be $\Delta v_{\rm th} = 1.0$ km s$^{-1}$. Since $\Delta v_{\rm th} \approx 0.5(T/100)^{1/2}$, with $T$ the temperature in the maser region, the $H_2O$ masers in the envelope of IRAS 19296+2227 exist at ∼400 K. Additionally, we find that the emerging brightness temperature of the strongest maser feature is $T_{\rm b}\Delta\Omega \approx 2.5 \times 10^9$ K sr. Because the maser is marginally resolved we take the size of the maser to be 0.3 mas. The measured brightness temperature of IRAS 19296+2227$f$ is thus $T_{\rm b} \approx 2 \times 10^{11}$ K. This implies a beaming solid angle $\Delta\Omega \approx 1.2 \times 10^{-2}$ sr, which is typical for the beaming angle of the $H_2O$ masers around evolved stars (Vlemmings et al. 2005). Finally, as detailed in Vlemmings et al. (2006a), the emerging brightness temperature implies that the masers are unsaturated.

### 4.2. Linear polarization

No linear polarization was detected from the IRAS 19296+2227 $H_2O$ masers down to ∼0.4%. This is a similar limit as found for the Mira and supergiant stars in our previous sample (Vlemmings et al. 2002, 2005). However, the strongest $H_2O$ maser of the PNe K3-35 was linearly polarized at a level of ∼1.6%. Unfortunately, the lack of good polarization angle calibration made it impossible to determine the polarization vector orientation. The fractional polarization of the K3-35 maser is similar to that found for $H_2O$ masers in star forming regions and those in the "water-fountain" PPNe source W43A (Vlemmings et al. 2006a; Vlemmings & Diamond 2006). Considering that the maser linear polarization fraction increases with maser saturation (e.g. Deguchi & Watson 1990), this seems to indicate that the saturation level of the $H_2O$ masers in the evolved stellar envelopes is on average less than that of the maser in star forming regions, PNe and related "water-fountain" sources.

### 4.3. The magnetic field of IRAS 19296+2227

The circular polarization of the strongest $H_2O$ maser feature ($f$) of IRAS 19296+2227 implies a magnetic field of $B_\parallel = -135 \pm 28$ mG in the $H_2O$ maser region. The field strength is similar to the fields previously detected using $H_2O$ maser polarization observations in the envelopes of evolved stars (Vlemmings et al. 2002, 2005, 2006b).

The origin of the magnetic field is unclear. As only one maser feature was strong enough to detect a magnetic field, a field local to the masers cannot be ruled out (e.g. Soker 2002). However, $H_2O$, OH and SiO maser polarization observations of a number of other evolved stellar sources reveal ordered large scale magnetic fields (e.g. Bains et al. 2003, 2004; Cotton et al. 2006; Kemball & Diamond 1997; Vlemmings et al. 2005, 2006b).

A field of 135 mG in a region with $T \approx 400$ K and a hydrogen number density $n_{\rm H_2}$ of ∼$10^9$ cm$^{-3}$, typical for $H_2O$ masers, implies that the ratio between magnetic and thermal pressure $B^2/(8\pi n_{\rm H_2} kT) \approx 15$. Assuming the masing material has a velocity of ≈3 km s$^{-1}$, the ratio between magnetic and dynamic pressure $B^2/(8\pi\rho v^2) \approx 5$, where $\rho$ and $v$ are the density and velocity of the maser medium. Thus, if the measured field strength in the IRAS 19296+2227 $H_2O$ maser region reflects a larger scale field, the magnetic field is strong enough to play an important role in the dynamics of the stellar outflow and possibly also in driving the mass-loss through the effects of Alfvén waves near the stellar surface (e.g. Falceta-Gonçalves & Jatenco-Pereira 2002; Vidotto & Jatenco-Pereira 2006).

## 5. Conclusions

We have measured a magnetic field of $B_\parallel = -135 \pm 28$ mG in the $H_2O$ maser region of the PPNe candidate star IRAS 19296+2227. The field strength is of the same order as the previously measured field strengths in evolved stellar envelopes. This implies that there is no significant evolution of the magnetic field in the transition from AGB star to early PNe. The magnetic field, if representative of the large scale field, is strong enough to play an important role in the dynamics of the stellar outflow and possibly also in driving the mass-loss. However a direct interpolation of the measured field strength to the stellar atmosphere is impossible.

While no linearly polarized $H_2O$ maser emission is detected in the envelope of IRAS 19296+2227, ∼1.6% fractional linear polarization is found for the strongest maser feature of the PNe K3-35, implying that the masers aree at least partially saturated. With sufficiently sensitive observations, the measurement of linear polarization of the $H_2O$ masers of PNe will enable us to probe the magnetic field morphology early in the PNe phase. The circular polarization measurement and lack of linear polarization suggests the $H_2O$ masers of IRAS 19296+2227 are unsaturated.

## References


Bains, I., Gledhill, T. M., Yates, J. A., & Richards, A. M. S. 2003, MNRAS, 338, 287
Bains, I., Richards, A. M. S., Gledhill, T. M., & Yates, J. A. 2004, MNRAS, 354, 529
Balick, B., & Frank, A. 2002, ARA&A, 40, 439
Bujarrabal, V., Castro-Carrizo, A., Alcolea, J., & Sánchez Contreras, C. 2001, A&A, 377, 868
Chevalier, R. A., & Luo, D. 1994, ApJ, 421, 225
Cotton, W. D., Vlemmings, W., Mennesson, B., et al. 2006, A&A, 456, 339
Deguchi, S., & Watson, W. D. 1990, ApJ, 354, 649
Engels, D. 1996, A&A, 315, 521
Etoka, S., & Diamond, P. 2004, MNRAS, 348, 34
Falceta-Gonçalves, D., & Jatenco-Pereira, V. 2002, ApJ, 576, 976
Frank, A., De Marco, O., Blackman, E., & Balick, B. 2007, [arXiv:0712.2004]
Herpin, F., Baudry, A., Thum, C., Morris, D., & Wiesemeyer, H. 2006, A&A, 450, 667
Imai, H. 2007, IAU Symp., 242, 279
Kemball, A. J., & Diamond, P. J. 1997, ApJ, 481, L111
Kemball, A. J., Diamond, P. J., & Cotton, W. D. 1995, A&AS, 110, 383
Kwok, S., Purton, C. R., & Fitzgerald, P. M. 1978, ApJ, 219, L125
Marvel, K. B., & Boboltz, D. A. 1999, AJ, 118, 1791
Miranda, L. F., Gómez, Y., Anglada, G., & Torrelles, J. M. 2001, Nature, 414, 284
Nedoluha, G. E., & Watson, W. D. 1992, ApJ, 384, 185
Soker, N. 2002, MNRAS, 336, 826
Suárez, O., Gómez, J. F., & Morata, O. 2007, A&A, 467, 1085
Vidotto, A. A., & Jatenco-Pereira, V. 2006, ApJ, 639, 416
Vlemmings, W. H. T., & van Langevelde, H. J. 2005, A&A, 434, 1021
Vlemmings, W. H. T., & Diamond, P. J. 2006, ApJ, 648, L59
Vlemmings, W. H. T., Diamond, P. J., & van Langevelde, H. J. 2002, A&A, 394, 589
Vlemmings, W. H. T., van Langevelde, H. J., & Diamond, P. J. 2005, A&A, 434, 1029
Vlemmings, W. H. T., Diamond, P. J., van Langevelde, H. J., & Torrelles, J. M. 2006a, A&A, 448, 597
Vlemmings, W. H. T., Diamond, P. J., & Imai, H. 2006b, Nature, 440, 58